LUND UNIVERSITY

Structural and optical characterization of Mg-doped GaAs nanowires grown on GaAs and Si substrates

Falcao, B. P.; Leitao, J. P.; Correia, M. R.; Soares, M. R.; Morales, F. M.; Manuel, J. M.; Garcia, R.; Gustafsson, Anders; Moreira, M. V. B.; de Oliveira, A. G.; Gonzalez, J. C.

Published in:
Applied Physics Reviews

DOI:
10.1063/1.4829455

2013

Link to publication

Citation for published version (APA):
Falcao, B. P., Leitao, J. P., Correia, M. R., Soares, M. R., Morales, F. M., Manuel, J. M., Garcia, R., Gustafsson, A., Moreira, M. V. B., de Oliveira, A. G., & Gonzalez, J. C. (2013). Structural and optical characterization of Mg-doped GaAs nanowires grown on GaAs and Si substrates. *Applied Physics Reviews*, *114*(18), [183508]. https://doi.org/10.1063/1.4829455

Total number of authors:
11

General rights
Unless other specific re-use rights are stated the following general rights apply:
Copyright and moral rights for the publications made accessible in the public portal are retained by the authors and/or other copyright owners and it is a condition of accessing publications that users recognise and abide by the legal requirements associated with these rights.
• Users may download and print one copy of any publication from the public portal for the purpose of private study or research.
• You may not further distribute the material or use it for any profit-making activity or commercial gain
• You may freely distribute the URL identifying the publication in the public portal

Read more about Creative commons licenses: https://creativecommons.org/licenses/

Take down policy
If you believe that this document breaches copyright please contact us providing details, and we will remove access to the work immediately and investigate your claim.

LUND UNIVERSITY

PO Box 117
221 00 Lund
+46 46-222 00 00

Download date: 07. Oct. 2022

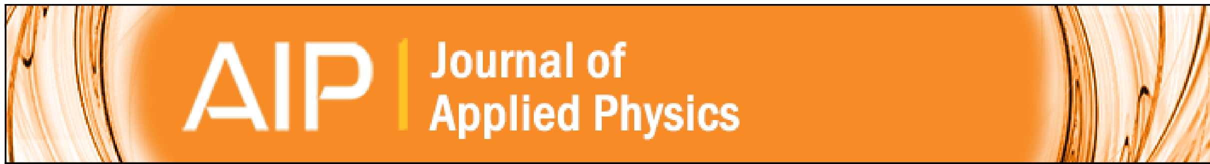

Structural and optical characterization of Mg-doped GaAs nanowires grown on GaAs and Si substrates

B. P. Falcão, J. P. Leitão, M. R. Correia, M. R. Soares, F. M. Morales, J. M. Mánuel, R. Garcia, A. Gustafsson, M. V. B. Moreira, A. G. de Oliveira, and J. C. González

Citation: Journal of Applied Physics **114**, 183508 (2013); doi: 10.1063/1.4829455
View online: http://dx.doi.org/10.1063/1.4829455
View Table of Contents: http://scitation.aip.org/content/aip/journal/jap/114/18?ver=pdfcov
Published by the AIP Publishing

Re-register for Table of Content Alerts

Create a profile.

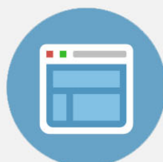

Sign up today!

[This article is copyrighted as indicated in the article. Reuse of AIP content is subject to the terms at: http://scitation.aip.org/termsconditions. Downloaded to] IP: 130.235.184.47 On: Sat, 08 Feb 2014 17:58:38

Structural and optical characterization of Mg-doped GaAs nanowires grown on GaAs and Si substrates

B. P. Falcão,[1,a)] J. P. Leitão,[1] M. R. Correia,[1] M. R. Soares,[2] F. M. Morales,[3] J. M. Mánuel,[3] R. Garcia,[3] A. Gustafsson,[4] M. V. B. Moreira,[5] A. G. de Oliveira,[5] and J. C. González[5]
[1]Departamento de Física, I3N, Universidade de Aveiro, Campus Universitário de Santiago, 3810-193 Aveiro, Portugal
[2]Laboratório Central de Análises, Universidade de Aveiro, 3810-193 Aveiro, Portugal
[3]Departamento de Ciencia de los Materiales e IM y QI, F. Ciencias, Universidad de Cádiz, 11510 Puerto Real (Cádiz), Spain
[4]Solid State Physics, The Nanometer Consortium, Box 118, Lund University, Lund SE-22100, Sweden
[5]Departamento de Física, Universidade Federal de Minas Gerais, 30123-970 Belo Horizonte, Minas Gerais, Brazil

(Received 13 August 2013; accepted 22 October 2013; published online 12 November 2013)

We report an investigation on the morphological, structural, and optical properties of large size wurtzite GaAs nanowires, low doped with Mg, grown on GaAs(111)B and Si(111) substrates. A higher density of vertical nanowires was observed when grown upon GaAs(111)B. Very thin zinc-blende segments are observed along the axis of the nanowires with a slightly higher linear density being found on the nanowires grown on Si(111). Low temperature cathodoluminescence and photoluminescence measurements reveal an emission in the range 1.40–1.52 eV related with the spatial localization of the charge carriers at the interfaces of the two crystalline phases. Mg related emission is evidenced by cathodoluminescence performed on the GaAs epilayer. However, no direct evidence for a Mg related emission is found for the nanowires. The excitation power dependency on both peak energy and intensity of the photoluminescence gives a clear evidence for the type II nature of the radiative transitions. From the temperature dependence on the photoluminescence intensity, non-radiative de-excitation channels with different activation energies were found. The fact that the estimated energies for the escape of the electron are higher in the nanowires grown on Si(111) suggests the presence of wider zinc-blende segments.
© 2013 AIP Publishing LLC. [http://dx.doi.org/10.1063/1.4829455]

I. INTRODUCTION

Semiconductor nanostructures have been emerging in many research fields as a consequence of the scientific progress and the ability to fabricate low-dimensional structures with tunable properties for each specific application. An exciting example is the growth of the wurtzite (WZ) crystalline phase in the usually stable zinc-blende (ZB) III–V semiconductors when scaling down from the bulk to the nanowire form.[1–4] Investigations have evidenced that the formation of the WZ phase is generally favored by processes arising from the large surface-to-volume ratios of the nanowires, usually with small diameters,[5,6] and its fraction along the growth axis depends on the growth parameters.[3,7–10] III–V nanowires have been grown by several techniques, namely, molecular beam epitaxy (MBE),[11–13] chemical beam epitaxy (CBE),[14,15] and metal-organic chemical vapor deposition (MOCVD)[2,16] through the particle-assisted vapor-liquid-solid (VLS)[17] mechanism mainly with Au as catalyst. Despite the significant achievements obtained in the nanowires synthesis, a full understanding of the influence of the substrate on the fraction of each phase is still lacking.[3,4,9,18–20] This is particularly important in the case of Si substrates if the goal is the integration on Si technology.

The alternating crystal structures along the nanowire's axis originate heterostructures with complex optical properties that requires a thorough investigation. It is generally accepted that WZ/ZB heterojunction in GaAs nanowires has a staggered type II band alignment where, under excitation, electrons (holes) are located in the ZB (WZ) side of the interface.[8,10,21,22] In the case of radiative recombination of these charge carriers, a spatially indirect radiative transition will occur. Meanwhile, the knowledge of several physical parameters is not well established and remains a controversial issue. For instance, theoretical values of the valence (ΔE_V) and conduction (ΔE_C) band offsets between the WZ and ZB phases in the range 76–122 meV and 53–117 meV, respectively, have been obtained.[10,23,24] Another disputed value is the band gap energy of WZ GaAs (E_g^{WZ}) where experimental reports and theoretical calculations support values either above[23,25–28] or below[10,22,24,29–31] the band gap energy of bulk GaAs (E_g^{ZB}). In addition to the coexistence of the two crystalline phases, other factors like orientation, dimension, substrate, and doping profiles influence the structural, optical, and electrical properties of the nanowires.[9,10,19,25,32]

Several studies performed on GaAs nanowires by photoluminescence (PL) have shown that at low temperature, the observed PL spectra are dominated by an emission in the energy range 1.42–1.55 eV characterized by many components.[8,10,33,34] The emission above ~1.52 eV has been ascribed by several authors[25,27,35] to the free-exciton/electron-hole recombination in pure WZ GaAs, implying that $E_g^{WZ} > E_g^{ZB}$, although a possible influence of quantum

a)Electronic mail: bfalcao@ua.pt

 © 2013 AIP Publishing LLC

[This article is copyrighted as indicated in the article. Reuse of AIP content is subject to the terms at: http://scitation.aip.org/termsconditions. Downloaded to] IP: 130.235.184.47 On: Sat, 08 Feb 2014 17:58:38

confinement effects could compromise that picture.[36] The fraction of each crystalline phase plays a strong role on the observed emission. For twinned and polytypic nanowires, several radiative transitions were observed in the range ∼1.42–1.50 eV. The works of Heiss *et al.*[10] and Spirkoska *et al.*[8,33] showed that in regions composed of either ZB or WZ phases, the spectra exhibit an emission peak close to the bulk GaAs band gap energy; while for regions consisting of random alternations of thin segments of ZB and WZ phases, the emission is redshifted.

Doping of GaAs nanowires is a field that has not been extensively investigated yet. However, their use in devices, in particular in solar cells, requires this problem to be more intensively addressed. At present, Be is the most commonly used p-type dopant in bulk GaAs due to its near-unity sticking coefficient and low vapor pressure at the usual growth temperatures used in MBE.[37–39] However, due to the high toxicity of Be, several attempts have been made to find nontoxic and noncarcinogenic alternatives. Mg is a promising one as it originates a shallow acceptor level in GaAs with an ionization energy of 28 meV.[40,41] Because of the low incorporation coefficient at the usual growth temperatures, it has been difficult to use Mg as a viable p-type dopant in GaAs.[39,42] Despite this limitation, we recently demonstrated the feasibility to grow GaAs:Mg nanowires.[36] This is a fundamental step for their use in solar cells if a p-n junction is intended to create an electric field to efficiently separate the charge carriers.[43,44]

In this work, we present a thorough investigation on the morphological, structural, and optical properties of Mg-doped GaAs nanowires, grown by MBE on two different substrates (GaAs(111)B and Si(111)). The correlation found between these properties is discussed in depth. Transmission electron microscopy (TEM) measurements revealed large size nanowires dominated by the WZ phase with a low density of thin ZB segments, which is uncommon for such large nanowires. In spite of being a macro experimental technique, grazing incidence X-ray diffraction (GID), performed for very low angles, confirm the TEM results. Systematic excitation power and temperature dependencies of the PL were performed. The observed radiative transitions for the nanowires grown in both substrates are clearly identified as type-II transitions. A strong correspondence between the activation energies of de-excitation non-radiative channels and the structure of the grown nanowires was found.

II. EXPERIMENTAL

A. Samples

GaAs nanowires were synthesized in a Riber 2300 R&D MBE reactor by applying the well known Au-assisted VLS growth mechanism. In order to understand the role of the substrate on the morphological, structural, and optical properties, two samples were produced, one grown on GaAs(111)B (sample A) and another grown on Si(111) (sample B). Prior to growth, the substrates were drop-coated with Au colloidal nanoparticles with an average diameter of 5.0 ± 0.5 nm. The growth was performed at 625 °C during 90 min, with an As_4 beam equivalent pressure (BEP) of 3.8×10^{-5} Torr, a Ga BEP of 7.2×10^{-7} Torr and at a nominal growth rate of 1 monolayer (ML)/s (estimated for an epitaxial layer). The p-type doping was achieved by keeping the Mg effusion cell at 175 °C. A nominal free hole concentration of 2×10^{16} cm^{-3} was determined by carrying out Hall effect measurements in a GaAs epilayer grown under the same growth conditions on a non-coated substrate. Such low doping concentrations are very difficult to measure in nanostructures. However, preliminary electrical measurements made on field effect transistors of individual highly Mg-doped GaAs nanowires have shown the p-type nature and a free hole concentration similar to the nominal value.

B. Characterization

The morphology of the nanowires was investigated by scanning electron microscopy (SEM) using a high performance Schottky field emission HR-FESEM Hitachi SU-70 microscope equipped with an in-lens secondary-electron and backscattered-electron detectors. The crystalline structure of the nanowires was investigated by transmission electron microscopy (TEM), which were previously mechanically removed from the substrates and deposited into holey carbon grids. A JEOL JEM-2011 (LaB_6 thermionic electron source) and a JEOL JEM 2010-FEG (LaB_6 field effect electron source) 200 kV-high resolution electron microscopes, with maximum resolution values of 2.3 Å and 1.9 Å, respectively, were used to achieve both low magnification and high resolution (HR) TEM images, as well as electron diffraction patterns of the GaAs nanowires. The crystalline structure of the nanowires was also inspected by grazing incidence GID measurements carried out on a PANalytical X'Pert MRD and MPD diffractometers using the Cu-$K_\alpha = 1.540598$ Å line. The study of the epitaxial layer underneath the nanowires was performed on a piece of sample A where the nanowires were mechanically removed with a razor blade.

Cathodoluminescence (CL) and PL spectroscopy were used to investigate the optical properties of the nanowires. The CL studies were performed in a dedicated setup with a SEM microscope (Cambridge Instruments 250) equipped with a liquid helium cold stage. Monochromatic images and spectra were recorded using a GaAs photomultiplier tube. The experimental conditions used were typically an electron accelerating potential of 5 kV with a probe current of 10 pA and the sample was kept at 7–8 K. The PL measurements were carried out in a Bruker IFS 66v Fourier Transform Infrared (FTIR) spectrometer equipped with a liquid nitrogen cooled Ge diode detector. The samples were inserted in a helium gas flow cryostat that allowed varying the temperature in the range 4–300 K. The excitation source was the 457.9 nm line of an Ar^+ ion laser with a power in the range 50–350 mW measured at the front of the cryostat window.

III. RESULTS AND DISCUSSION

A. Morphology and crystalline structure

Topographical SEM images (Fig. 1) show a mesh of tangled non-vertical nanowires with very large dimensions. Favored by the long time of growth,[16] its lengths extend up to a few tens of micrometers and the diameters vary from

[This article is copyrighted as indicated in the article. Reuse of AIP content is subject to the terms at: http://scitation.aip.org/termsconditions. Downloaded to] IP: 130.235.184.47 On: Sat, 08 Feb 2014 17:58:38

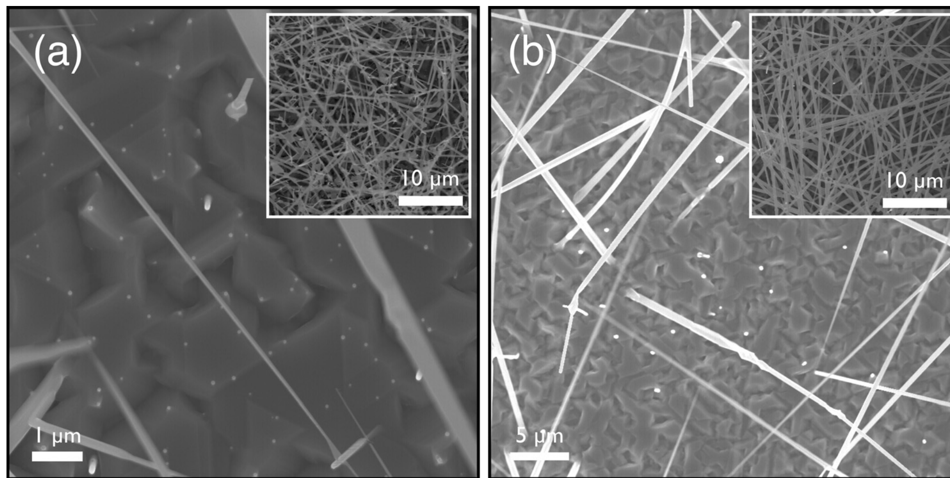

FIG. 1. Scanning electron microscopy images of Au-catalysed GaAs:Mg nanowires grown on: (a) sample A (GaAs(111)B substrate) and (b) sample B (Si(111) substrate). The bright spots correspond to vertical nanowires with diameters of a few tens of nanometers. Low magnification images are shown on the top right insets.

several hundreds of nanometers at the base to a few tens of nanometers at the tip. Although it is not clear in these images, a close inspection reveals a manifold of growth directions characterized by specific values of angles. The lack of a direct epitaxial relation with the substrate can be understood given the formation of polycrystalline seeds by three-dimensional twinnings at the initial growth stages.[45,46] Notwithstanding, smaller and vertical oriented nanowires (with diameters in the order of a few tens of nanometers) are observed on both samples (bright spots), with a higher density on sample A (GaAs(111)B substrate). This is a clear indication of a direct epitaxial relation with the substrate in which the nanowires are grown. In the case of the Si(111) substrate, it is not surprising a lower density since the growth yield along the vertical direction on a (111) surface can be largely determined by the lattice mismatch at the nanowire-substrate interface.[46,47] Finally, we would like to stress out that cross-sectional SEM images (not shown) revealed the presence of an epitaxial GaAs thin layer underneath the nanowires (few tens of nanometers), and with a higher thickness outside the Au-coated areas (several hundreds of nanometers).

Low magnification TEM images exhibit the presence of transversal stacking defects unevenly distributed along the nanowires, as can be seen in Figs. 2(a)–2(d) (stripes contrasting with the rest of the nanowire). The planar nature of these

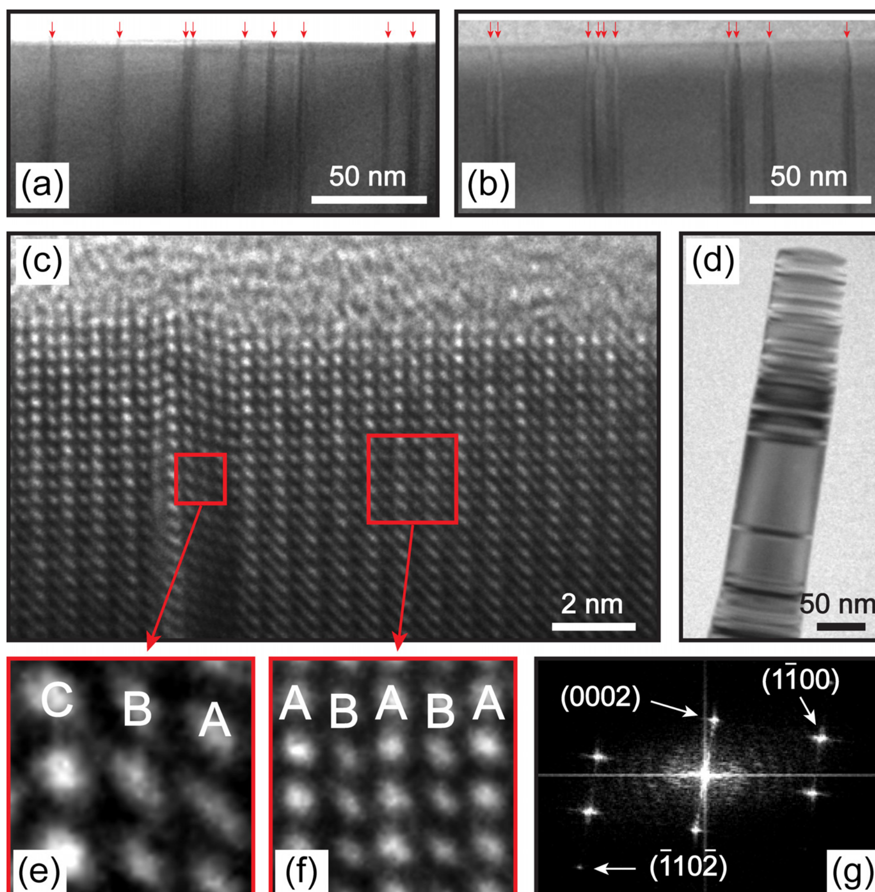

FIG. 2. Bright Field TEM images of GaAs nanowires from (a) sample A and ((b) and (c)) sample B. (c) HRTEM image of a nanowire from sample B and details of: (f) matrix and (e) ZB segments. (g) Fast Fourier transform of a HRTEM image of a thick region and the respective crystallographic indexes of the diffraction spots. The collection direction is the hexagonal $[11\bar{2}0]$ zone axis in images (a)–(c); and $[1\bar{1}00]$ direction in image (d), which shows that the nanowire growth axis occurs along the [0001] hexagonal direction. Some astigmatism is observed in (c), which does not affect the conclusions about it.

[This article is copyrighted as indicated in the article. Reuse of AIP content is subject to the terms at: http://scitation.aip.org/termsconditions. Downloaded to] IP: 130.235.184.47 On: Sat, 08 Feb 2014 17:58:38

defects is clearly confirmed by: (i) the fact that they are resolvable for orientations perpendicular to the nanowires axis ($[11\bar{2}0]$ zone axis for Figs. 2(a)–2(c), $[1\bar{1}00]$ for Fig. 2(d)); and (ii) high resolution TEM (HRTEM) images (see Fig. 2(c)) show that they are formed by few bilayers of GaAs (occasionally, a twin boundary is observed). The linear density of these defects, obtained through the ratio between its number in the nanowire and the length of that nanowire, were found to be $12.6\,\mu\mathrm{m}^{-1}$ and $15.5\,\mu\mathrm{m}^{-1}$ in the case of nanowires grown on GaAs(111)B and on Si(111), respectively. This result suggests that the Si(111) substrate leads to a decrease of the crystalline homogeneity of the nanowires.

The crystalline structure of several nanowires from both samples was evaluated by selected area electron diffraction (SAED) patterns and HRTEM images, performed on regions of different diameters of the nanowires. Fig. 2(c) shows the atomic arrangement in the thinnest part of a nanowire grown on GaAs(111)B (results are identical for all studied nanowires from both samples). Details of HRTEM micrographs reveal that the nanowire is formed by a matrix with an ABAB stacking sequence characteristic of a 2H-polytype hexagonal WZ crystal structure (Fig. 2(f)).[48] These results are in good agreement with the features observed in SAED patterns where, for a statistically significant number of nanowires and a large field of view, only the hexagonal crystalline structure was observed. On the other hand, the defects present the ABCABC atomic arrangement characteristic of the (3C) ZB crystal structure (Fig. 2(e)).[48]

The nanowires thicker regions were also characterized. High resolution is only possible to be achieved from the edges of the nanowires, and even there the resulting images do not lead to a direct conclusion about the nanowires crystalline structure. Nevertheless, the Fast Fourier transform of several HRTEM images in these regions show, for a relatively wide field of view and the hexagonal $[11\bar{2}0]$ zone axis, the typical rectangular shape formed by the arrangement of the reflections, as it is presented in Fig. 2(g). Hence, there is evidence for a dominance of the WZ phase in these nanowires, even in the larger ones, while the ZB phase appears only in the form of very thin segments (i.e., in faulty regions of the hexagonal phase). As will be seen ahead, the mixed structure along the nanowires plays a major role in their optical properties.

The crystalline phases on the nanowires were also investigated by XRD measurements in the grazing incidence configuration as it considerably reduces the contribution from the epitaxial GaAs layer underneath the nanowires. In Fig. 3, we show the GID diffractograms probed with an incident angle $\omega = 2^\circ$, and the positions and relative intensities for the reflections related to both crystalline phases according to the database of the ICDD.[49,50] We must mention that while for the ZB phase these reflections are well known, for the WZ phase, we only found one theoretical work[51] that predicts their positions and relative intensities. For both samples, we observe two sets of reflections: (i) one related to the ZB phase, and (ii) another consisting of peaks close to the theoretical positions of the WZ reflections but shifted to lower 2θ values. Some reflections from the ZB and WZ phases are overlapped. The presence of the WZ phase in the nanowires is confirmed by similar GID measurements performed on a piece of sample A after the removal of the nanowires, which shows the absence of all WZ related peaks (see Fig. 3). In fact, for the latter diffractogram, just reflections of the ZB phase are observed, which come from the epitaxial layer underneath the nanowires.

In order to minimize as much as possible the contribution from the epitaxial layer to the measured diffractogram,

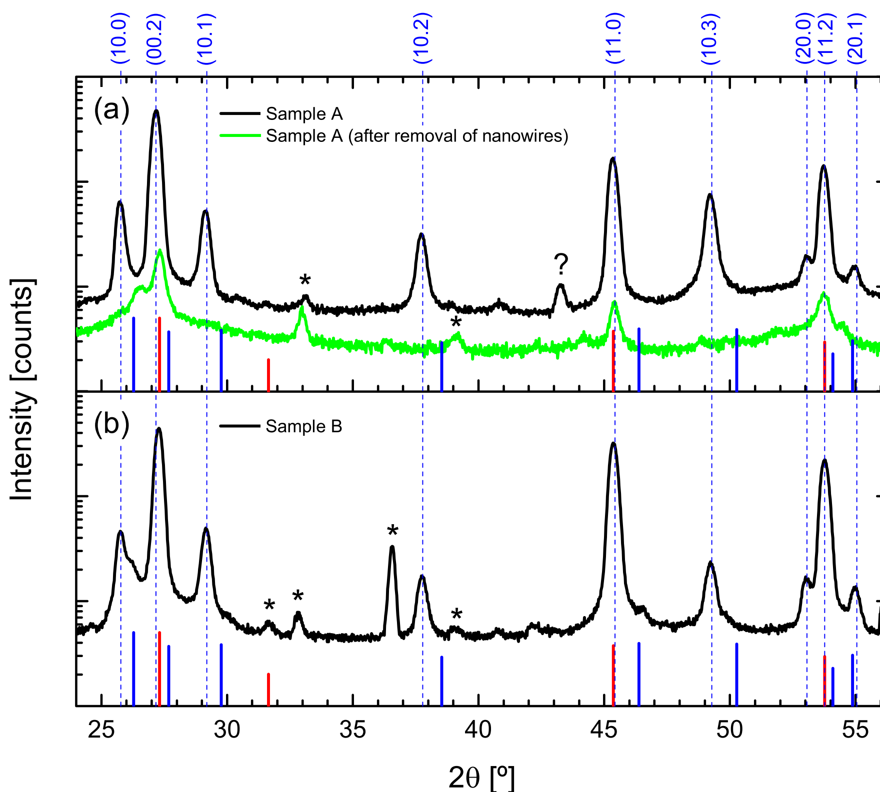

FIG. 3. (a) Comparison of GID diffractograms from sample A prior to (black) and after (green) the removal of nanowires. (b) GID diffractogram from sample B. In both figures, the red (blue) vertical bars illustrate the expected positions and relative intensities of the ZB (WZ) reflection peaks accordingly to ICDD entries.[49,50] The dashed lines reflect our attribution for the angles of the WZ related reflections, identified in accordance to the (hk.l) crystallographic notation for hexagonal structures. The peaks ⋆ comes from residues on the base of the samples from the glue used to fix the sample inside the growth chamber.

[This article is copyrighted as indicated in the article. Reuse of AIP content is subject to the terms at: http://scitation.aip.org/termsconditions. Downloaded to] IP: 130.235.184.47 On: Sat, 08 Feb 2014 17:58:38

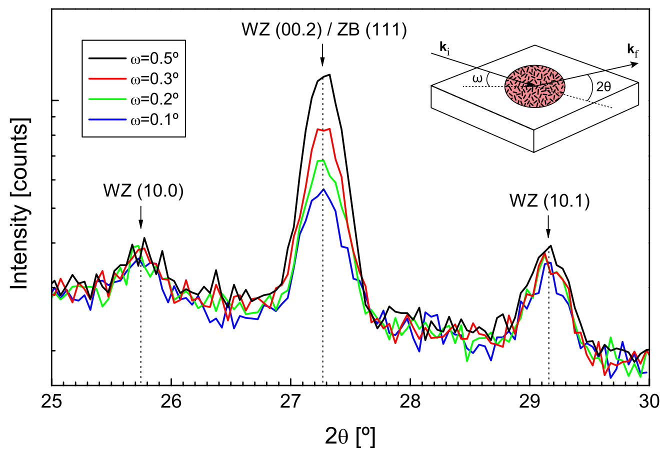

FIG. 4. GID diffractograms obtained from sample B as a function of the incidence angle ω. The top right inset illustrates the $2\theta/\omega$-scan experimental setup.

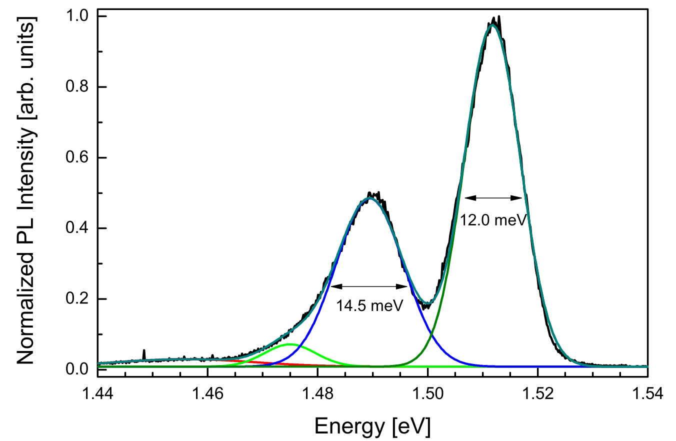

FIG. 5. CL spectrum measured at 8 K from the GaAs:Mg epilayer of sample A.

we reduced the incident angle ω from 0.5° to 0.1° in GID measurements for sample B (see Fig. 4). The peaks at $2\theta \sim 25.7$, 29.2° are assigned to reflections in the WZ planes (10.0) and (10.1), whereas the peak at $2\theta \sim 27.3°$ has contributions from atomic planes (00.2) in WZ and (111) in ZB.[49,50] For the first two peaks, just related to the WZ phase, no significant dependence on ω is observed for the relative intensity. This is an evidence that for all ω-scans, approximately the same amount of material in the WZ phase is being analysed. On the other hand, the relative intensity of the peak at $2\theta \approx 27.3°$ clearly diminishes with decreasing ω, approaching the relative intensities of the other two WZ related peaks. The theoretical calculations[51] previously mentioned foresee close relative intensities for the WZ related peaks in the range 25°–30° (see the blue vertical bars in Fig. 3). Due to the low signal-to-noise ratio and low angular resolution of the diffractograms, the deconvolution of the contributions to this peak, from each phase, is not possible, hindering the quantification of the contributions of the ZB (111) atomic planes from the nanowires and the GaAs epilayer. In spite of that we consider that the main contribution to the reflection peak at $2\theta \approx 27.3°$ comes from the WZ (00.2) atomic planes, though the ZB contribution from the epilayer cannot be completely excluded. These XRD results support the previous conclusion that WZ is the dominant crystalline phase in these nanowires. Additionally, they show the feasibility of grazing incidence measurements, at very low angles, for a qualitative evaluation of the crystalline phases in GaAs nanowires.

B. Luminescence from the GaAs:Mg epilayer

Before the discussion of the results for the nanowires, it is important to discuss briefly the luminescence from the GaAs:Mg epilayer, in view of its possible influence on the recorded nanowires emission. PL was unable to measure the emission from the epilayer, even under high excitation power. However, luminescence from this layer could be measured in CL due to the higher excitation density.[52] In Fig. 5, we show the spectrum measured at ~8 K in a region uncoated with Au nanoparticles, where only growth of the epilayer occurred. The spectrum is dominated by two bands that are well fitted by two Gaussian curves, whose peaks are located at ~1.490 and ~1.512 eV and have a full-width at half-maximum (FWHM) of 14.5 and 12.0 meV, respectively. The latter band is ascribed to radiative recombinations of free excitons and bound excitons to shallow neutral donors (D^0X) and acceptors (A^0X) in GaAs.[53,54] Due to the insufficient spectral resolution, it is not possible to distinguish them. Concerning the peak at ~1.490 eV, its spectroscopic shift from the ZB band gap energy is ~29 meV, very close to the binding energy of an exciton to the Mg acceptor in bulk GaAs.[38,41,54] Given the intentional doping with this impurity, which was confirmed by Hall effect measurements ($p = 2 \times 10^{16}\,\mathrm{cm}^{-3}$) performed on epilayers grown in similar conditions, we attribute this band to the radiative recombination of an exciton bound to the Mg acceptor.

C. Luminescence from the nanowires

We start by presenting a series of monochromatic CL images from the bottom part of a nanowire in which the emission was analysed for a few values of energies in the range ~1.45–1.49 eV (Fig. 6). As seen in each image, the nanowire has a striped emission along its growth axis. We must note that due to the insufficient spatial resolution, the axial length of the strips can look longer than the actual length of the luminescent segments. Their observation for particular values of energy suggests that the crystal structure is playing a major role in the trapping of charge carriers and subsequent radiative recombination.

The occurrence of ZB segments in nanowires dominated by the WZ phase, as evidenced by the structural characterization, creates several interfaces between distinct phases in which the band alignment is of type II.[8,10,21,23] Upon excitation, electrons and holes are trapped in the ZB and WZ segments, respectively. As suggested by the spread of the CL emission, we expect that the presence and distribution of these ZB segments along the nanowires axis influence the radiative recombination mechanisms, as will be discussed below. Other defects including impurities, namely the Mg acceptors, can also create additional radiative recombination channels.

It is important to note that PL is a macro experimental technique that probes simultaneously several hundreds of

[This article is copyrighted as indicated in the article. Reuse of AIP content is subject to the terms at: http://scitation.aip.org/termsconditions. Downloaded to] IP: 130.235.184.47 On: Sat, 08 Feb 2014 17:58:38

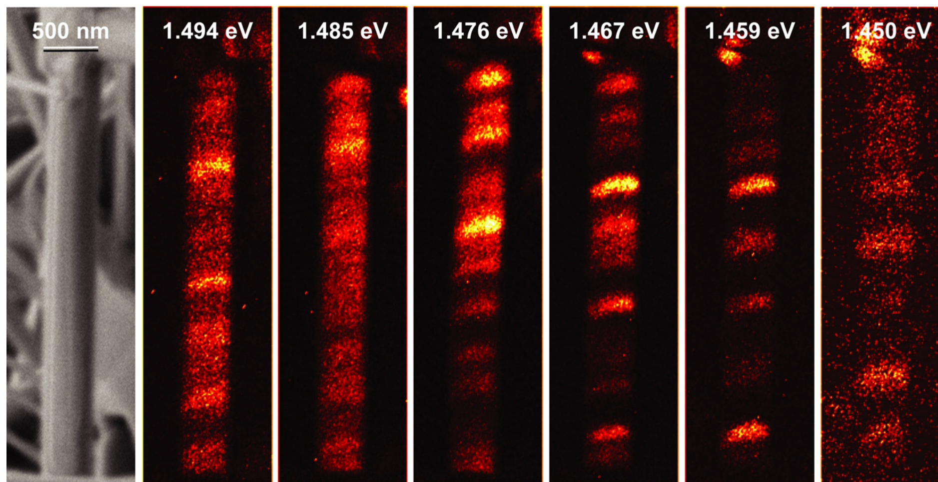

FIG. 6. CL images at 8 K from a single nanowire of sample A emitting at different energies, as indicated on top of each image; dark represents no emission and yellow the regions where the CL intensity is highest. The SEM image of the measured part of the nanowire is shown on the left.

nanowires. The PL spectra at low temperature for both samples are shown in Fig. 7. In the case of sample A, the spectrum shows an emission in the range ~1.25–1.52 eV dominated by a band located at ~1.48 eV. Additionally, a few transitions with low relative intensities can be identified in the low energy side. For sample B, the spectrum exhibits mainly an asymmetric broad emission in the range ~1.40–1.51 eV with two peaks located at ~1.46 and ~1.48 eV with comparable relative intensities. Following a common procedure, in order to analyse the observed emission, the spectra were fitted with several Gaussian components. The model for each sample considers the lowest number of components needed to fairly well reproduce the measured spectra for all excitation powers and temperatures studied in this work. For both samples, in the low energy side of the spectra, the reduced PL intensity was fitted with a very broad component located at ~1.35 eV. The model for sample A considered six additional components; whereas for sample B, just three components were considered. In view of an extended comparison of the emission from the nanowires, we will restrict our analysis to the region ~1.42–1.52 eV where the relative PL intensity is higher and which is in accordance with our CL results and reported PL from polytypic GaAs nanowires.[8,10,33] This analysis corresponds to components labeled A_1–A_3 (sample A) and B_1–B_2 (sample B). The emission below ~1.44 eV has a low relative intensity and is likely related to deep defects.

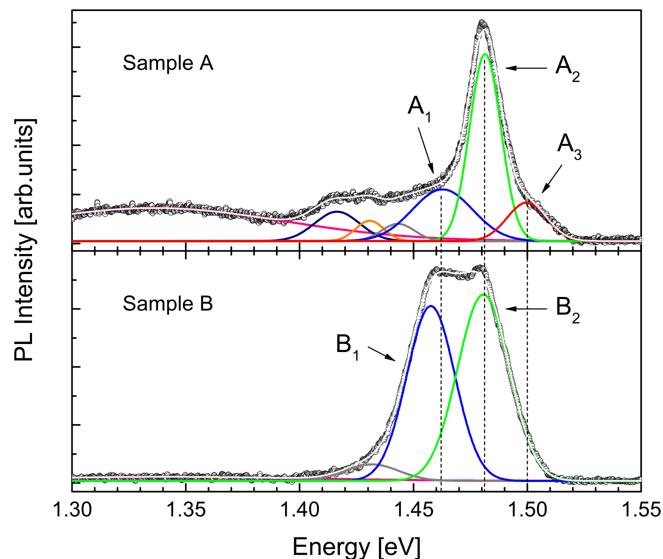

FIG. 7. PL spectra of GaAs:Mg nanowires measured at ~4.5 K for sample A (GaAs(111) B substrate) and sample B (Si(111) substrate). The emission in both spectra was fitted with Gaussian components.

At this point, we must note that for both samples, the PL was measured on bare nanowires. Contrary to previous studies[10,22,28,34,55] where the nanowires were covered by an (Al,Ga)As shell to enhance the luminescence efficiency, in our samples, it was high enough to allow a thorough PL investigation. Tomioka *et al.*[55] also pointed that the Si(111) substrate critically influences the optical properties due to the presence of defects. In our case, even for the growth on the Si(111) substrate, we observe a signal-to-noise ratio comparable to the one of sample A in the same spectral region (see Fig. 7).

D. Nature of the radiative transitions

The excitation power (P) dependence of the near band edge PL has been widely used to discuss the nature of the radiative transitions in luminescence studies of bulk semiconductors and heterostructures. However, for GaAs nanowires, such studies are lacking in the literature. In this work, the range of P values investigated was around one order of magnitude due to a compromise between the observation of the nanowires related emission and their structural integrity. We started by studying the dependence on P of the integrated PL intensity (I) for the Gaussian components A_1–A_3 and B_1–B_2. As can be seen in Fig. 8, the experimental behavior of log(I) vs log(P) follows a linear dependence that is well described by a

$$I \propto P^m \quad (1)$$

law, where m is an adjustable parameter that represents the slope in a log(I)–log(P) plot. Fits to the experimental points for all components of both samples reveal values of m lower than unity (see Table I). According to Schmidt *et al.*,[56] luminescence lines whose fits are parameterized by $m < 1$ are not of excitonic nature. On the other hand, values lower than the unity

[This article is copyrighted as indicated in the article. Reuse of AIP content is subject to the terms at: http://scitation.aip.org/termsconditions. Downloaded to] IP: 130.235.184.47 On: Sat, 08 Feb 2014 17:58:38

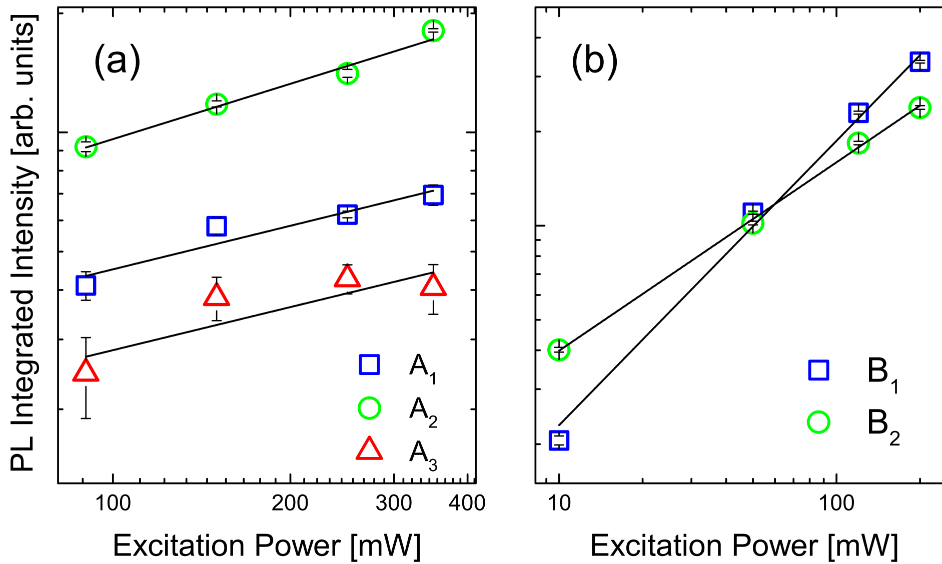

FIG. 8. log(I)–log(P) plots for (a) sample A and (b) sample B. The fits to the experimental points were obtained with Eq. (1).

are also compatible with type II transitions at the interfaces between the quantum well and the barriers, as has been discussed by other authors, for instance, for the WZ/ZB heterointerface in GaN nanowires[57] and for the Si/Ge system.[58–61]

To clarify the physical origin of the transitions observed in this work, let us consider the peak energy vs. $P^{1/3}$ plots shown in Fig. 9. In spite of the reduced number of experimental points, globally all components exhibit a blue shift with the increase of P. The evidenced linear behavior is in accordance with the analysis of the dependence on the photoexcitation of the density of non-equilibrium charge carriers that shows a proportionality of the ground state energy for electrons, E_c, with P given by[62]

$$E_c \propto P^{1/3}. \quad (2)$$

This trend is characteristic of type II radiative transitions[63–66] and can be understood as follows: upon excitation, as electrons and holes are localized on different sides of the interface between ZB/WZ segments (in our case), dipole layers are formed causing an electric field. For high values of P, the electric field is increased and a bending of the valence and conduction bands occurs with a consequent appearance of a Hartree potential. Consequently, the energy levels for the charge carriers (electrons) in the thin (ZB) segments suffer a blue shift. Additionally, the large excess of carrier densities characteristic of high P values will result in the filling of the higher energy states. Both effects contribute to a shift of the energy of the radiative transition to higher energies, as experimentally observed.[58,67]

In the case of component B_1, some spreading of the experimental points is observed. This could be due to the difficulties in fitting the spectra and/or to the limits of application of the 1/3 power-law fitting over a limited range of excitation densities as stated by Jo *et al.*[68] Whatever the case, the compatibility of this component with a type II radiative transition is not ruled out.

As discussed in the literature, the energy of the radiative recombination of both types of carriers in the same spatial region (type I transitions) will also suffer a blue shift with the increase of P.[69–71] However, the expected dependence of the peak energy on the excitation power does not obey a $P^{1/3}$ law.[70,71] Additionally, the estimated values for m in Eq. (2) are clearly higher than those obtained in this work. Consequently, the occurrence of type I transitions should be excluded in the present case. Actually, considering the commonly accepted band offset at the WZ/ZB heterointerface, just a type II heterostructure should be present in these nanowires, which is compatible with the previous discussion.

These results bring further confirmation on the occurrence of the type II radiative transitions in polytypic GaAs nanowires, as has been pointed in several works.[8,10,21,22] The possible involvement of defect states in the WZ side, namely Mg impurities, cannot be ruled out. However, even in that case, the observed transitions would be of indirect nature in the real space.

TABLE I. Spectroscopic energies (E_p) and activation energies, with respective uncertainties, obtained from the fit of Eq. (3) to the temperature dependence of the relative intensities of the Gaussian components fitted to the PL spectra of samples A and B. The m parameter obtained from the fit of Eq. (1) to the data from the excitation power dependence is also presented.

Sample	Component	E_p (eV)	E_1 (meV)	E_2 (meV)	E_b (meV)	m
A	A_1	1.463 ± 0.001	1.7 ± 0.1	…	21 ± 4	0.36 ± 0.08
	A_2	1.482 ± 0.001	1.1 ± 0.2	…	10 ± 2	0.46 ± 0.05
	A_3	1.500 ± 0.001	1.2 ± 0.2	…	6.2 ± 0.9	0.4 ± 0.1
B	B_1	1.458 ± 0.001	8.4 ± 0.5	…	44 ± 10	0.91 ± 0.05
	B_2	1.481 ± 0.001	1.1 ± 0.5	6.2 ± 0.7	36 ± 12	0.60 ± 0.02

[This article is copyrighted as indicated in the article. Reuse of AIP content is subject to the terms at: http://scitation.aip.org/termsconditions. Downloaded to] IP: 130.235.184.47 On: Sat, 08 Feb 2014 17:58:38

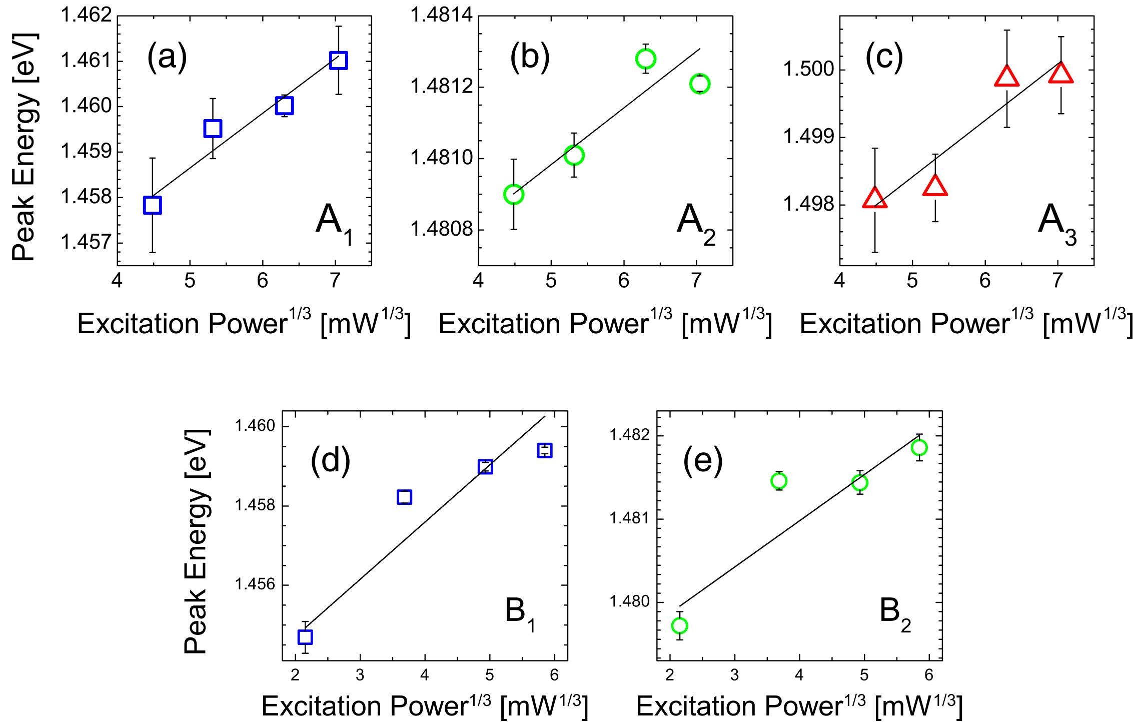

FIG. 9. Dependence on the excitation power of the PL peak energy of the Gaussian components that describes the near band edge luminescence of (a)–(c) sample A and (d)–(e) sample B. The fits to the experimental points were obtained with Eq. (2).

E. Non-radiative de-excitation channels

The temperature dependence of PL was investigated for both samples and the resulting spectra fitted with the models described previously (see Fig. 7). The obtained data for the (i) peak energy and the (ii) PL intensity of each Gaussian component as a function of T are plotted in Fig. 10. In the first case, with increasing T, all components (with the exception of B_2) shift to lower energies at a rate that roughly follows the temperature dependence of E_g^{ZB} (dashed line).[72] Concerning the evolution of the band gap energy of the WZ phase, Ahtapodov *et al.*[28] showed for WZ GaAs nanowires a close behavior to the one of E_g^{ZB} for approximately the same temperature range studied in this work. Either the case, the experimental behavior is consistent with the observations of Singh *et al.*[73] in which the temperature dependence of the peak energy of type II transitions follows the band gap variation of the quantum well and/or barrier materials. The blue shift of B_2 may be ascribed to the absence of a component in the high energy queue of the spectra. Although the fitting methodology was based on the assignment of the lowest number of components that reproduce the spectra, the shape of the spectra in this region (for all temperatures) did not show any clear evidence for an additional component. Recently, Graham *et al.*[34] described the PL from polytypic nanowires with an average volume fraction of the ZB structure of at least 80%, grown on SiO_2 coated GaAs(111)B substrates. The reported PL is dominated by a large band that was ascribed to emission from polytypic regions of the nanowires, and whose peak energy showed a S-shaped temperature dependence. This behavior was not observed in this work. With the exception of B_2, just a red shift is observed, in good agreement with the temperature dependence of E_g^{ZB}, thus further supporting the attribution of all studied components to the radiative recombination of electrons and holes at the ZB/WZ interface.

Concerning the dependence on T of the PL intensity, a strong quenching with increase of T is observed for all components. The experimental behavior can be understood considering the thermal activation of non-radiative de-excitation channels.[74] In general, with increasing T, the charge carriers can be released individually or in the form of an exciton from the radiative state to one or more discrete excited states, or to a band. The generic equation that describes the dependence on the temperature of the PL intensity is given by[74]

$$I(T) = I_0\left[1 + \sum_i c_i \exp\left(-\frac{E_i}{kT}\right) + c_b T^{3/2} \exp\left(-\frac{E_b}{kT}\right)\right]^{-1}, \tag{3}$$

where I_0 is the PL intensity at 0 K and k is the Boltzmann constant. The second term in the sum within parenthesis describes the existence of one or more discrete excited levels, each one parameterized by activation energies E_i, whereas the third term involves a band with its edge at an energy E_b from the radiative level. The factors c_i are parameters proportional to the ratio between the degenerescence of the respective excited state and of the radiative state, whereas $c_b T^{3/2}$ accounts for the effective density of states of the band involved and c_b is a fitting parameter.

Different models were tested in order to describe the thermal quenching of the PL intensity for each component. The fits of Eq. (3) to the experimental points are represented by the solid lines in Fig. 10 and the obtained activation energies are presented in Table I. In the case of sample A, the best fitting model considers two quenching channels, one

[This article is copyrighted as indicated in the article. Reuse of AIP content is subject to the terms at: http://scitation.aip.org/termsconditions. Downloaded to] IP: 130.235.184.47 On: Sat, 08 Feb 2014 17:58:38

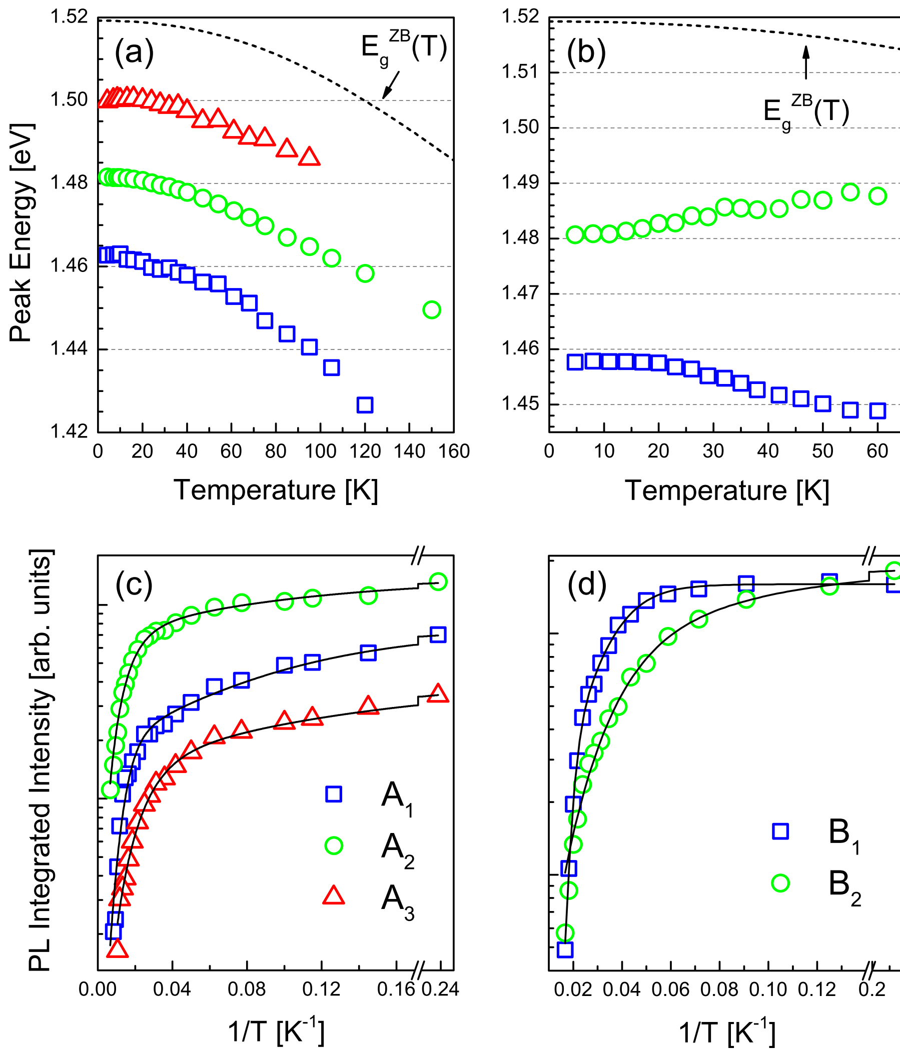

FIG. 10. Dependence on temperature of the ((a) and (b)) peak energy and ((c) and (d)) PL intensity of the near band edge emission of sample A ((a) and (c)) and sample B ((b) and (d)). The dashed line $E_g^{ZB}(T)$ represents the temperature dependence of the band gap energy of the ZB GaAs.[72] The fits to the experimental points in the Arrhenius plots ((c) and (d)) were obtained with Eq. (3).

involving a discrete excited level and the other a band. The first one is observed in the low temperatures regime and was parameterized by very low activation energies (1.1–1.7 meV), whereas the channel involving the band is observed for higher temperatures and the resulting activation energies are in the range ∼6–21 meV. For sample B, the best model for component B_1 comprises the thermal activation of two non-radiative de-excitation channels, one involving a discrete energy level ($E_1 = 8.4 \pm 0.5$ meV) and the other, a band ($E_b = 44 \pm 10$ meV). For component B_2, the experimental behavior requires the existence of two discrete levels, with activation energies of 1.1 ± 0.5 and 6.2 ± 0.7 meV, and a channel associated with a band for which an activation energy of 36 ± 12 meV was obtained. For both samples, the value of E_b decreases as the corresponding PL component occurs at higher spectroscopic energies.

The comparison of all activation energies for the different non-radiative channels shows that for sample A, the energy separation of the discrete energy level to the radiative state is very small (<2 meV). In sample B, we identified a channel involving a discrete energy level with an energy separation to the radiative state of several meV (∼6–8.5 meV). Regarding the channel involving a band, we must note that the corresponding activation energy describes the complete release of a carrier from the optical center. The fits revealed lower activation energies for sample A than for sample B meaning that, in the last sample, the depth of the radiative state relatively to the band is larger. In the scope of type II radiative transitions, the above de-excitation mechanism should consist of the release of the confined charge carrier to the corresponding band at the barrier, i.e., release of electrons confined in the ZB segments to the WZ conduction band. In Fig. 11, we present an energy diagram that illustrates the band alignment in WZ dominated nanowires with very thin ZB segments. Due to the very low thicknesses estimated for the ZB segments, the electron (and also hole) levels are not the bulk energy levels expected for a thick segment (dashed lines in Fig. 11). Upon excitation, the electrons are confined in the ZB segments and the holes are in the WZ side of the interface. The thermal release of the electrons is parameterized by the E_b energy whereas the de-excitation mechanism involving the discrete excited state (parameterized by the energy E_1) is represented by an hypothetical non-radiative defect (NRD) on a WZ segment. This discrete energy level can be an excited state of the radiative optical center or it may be created by other defect in the sample.

The above discussion for the activation energies involving the thermal ionization of the optical center suggests that the ZB segments should have a larger thickness in sample B (Si(111) substrate). Such increase of activation energies with

[This article is copyrighted as indicated in the article. Reuse of AIP content is subject to the terms at: http://scitation.aip.org/termsconditions. Downloaded to] IP: 130.235.184.47 On: Sat, 08 Feb 2014 17:58:38

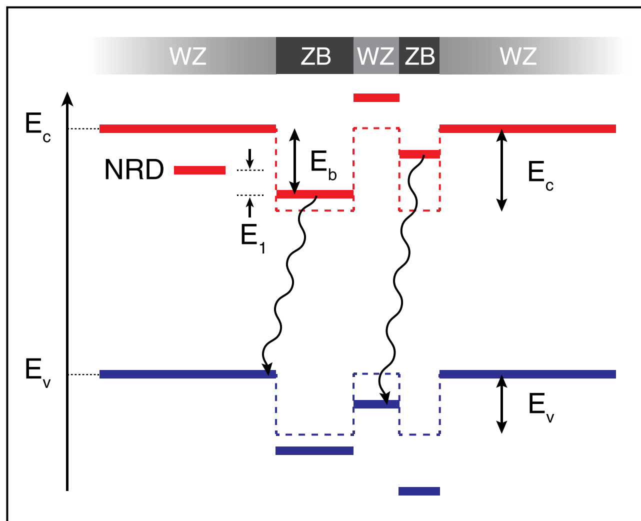

FIG. 11. Energy-level scheme of nanowire with WZ and ZB phases. At a very low temperature, the blue (red) energy levels are occupied (unoccupied) by electrons. The dashed lines represent the conduction and valence bands for both bulk phases. The fundamental energy levels inside the potential wells are shifted to higher energies due to quantum confinement. The curved arrows represent type II radiative transitions under excitation. NRD represents an hypothetical defect level in the WZ phase. The energies E_1 and E_b correspond to activation energies of non-radiative de-excitation channels discussed in the scope of Eq. (3).

the enlargement of the potential wells will be reflected on lower radiative recombination energies, as shown in Fig. 11 and as observed experimentally for type II transitions in InP/GaAs ultrathin quantum wells.[73] Indeed, we observed a slight red shift of the emission for the growth on Si(111)substrate, as well as an increase of the relative intensity of the radiative transitions that are modeled by B_1 (at lower spectroscopic energies). These results support that the ZB segments in sample B are thicker and are present at a higher linear density. This interpretation agrees with the findings of other authors,[8,10,22] which showed that for polytypic GaAs nanowires, with the increase of the alternation of both phases, the emission suffers a redshift. Therefore, the different components observed in the PL spectra from both samples should be related with the distribution of sizes of the ZB segments and with their linear density along the nanowire. These results suggest a clear influence of the substrate on the nanowires structure, which is reflected on the electronic levels structure of the nanowires.

F. Considerations about the Mg doping

Regarding the possible influence of Mg acceptors related luminescence in the nanowires, it must be noted that all identified Gaussian components showed a behavior compatible with a type II transition. No clear experimental evidence was obtained for the involvement of Mg. Two explanations can be given for that. On one hand, a relatively low efficiency in the capture of charge carriers or excitons by the Mg acceptors in comparison to the localization of charges at the ZB/WZ interface could occur. Additionally, the Mg related emission might also be masked by the emission from the mixed crystal structure, as both overlap. The mixed crystal structure results in emission in the range from 1.43 to 1.51 eV; (Ref. 8) and from the CL study of the epilayer in Fig. 5, we observed Mg related emission at 1.49 eV. On the other hand, as already discussed, we cannot exclude the possibility that the hole in the WZ barrier could be bound to a Mg acceptor. However, in this case, the nature of the radiative transition is dominated by the type II character, which justifies the experimental results, namely the excitation power dependence.

IV. CONCLUSIONS

An investigation of morphological, structural, and optical properties of Mg-doped GaAs nanowires, grown by MBE on GaAs(111)B and Si(111) substrates, was presented. For both substrates, vertical and non-vertical nanowires were observed. The vertical ones have diameters of the order of a few tens of nanometers and their density is higher on the GaAs(111)B substrate. The tangled non-vertical nanowires have diameters varying from several hundreds of nanometers at the base to a few tens of nanometers at the tip, and lengths up to a few tens of micrometers. The crystalline structure is dominated by the WZ phase with very thin ZB segments along the growth axis. The dominance of the WZ phase is uncommon for nanowires with such large sizes. TEM revealed a mean linear density of ZB segments (obtained through the ratio between its number in the nanowire and the length of that nanowire) of 12.6 μm^{-1} and 15.5 μm^{-1} for the growth on GaAs(111)B and Si(111) substrates, respectively, which is evidence for the role of the substrate on the crystalline homogeneity of the nanowires.

The efficiency of the luminescence was high enough in spite of being originated on GaAs nanowires not covered by an (Al,Ga)As passivation layer. The existence of alternating segments of both crystalline phases along the axis has a strong influence on optical properties. Both CL and PL measurements showed emission in the range ~1.40–1.52 eV. The dependence on the excitation power of the PL shows that the observed radiative transitions are of type II at the interface between WZ and ZB segments. The increase of temperature results on a red shift of the PL in accordance with the shrinkage of the ZB GaAs band gap energy. Two non-radiative PL quenching channels were identified for almost all radiative transitions, one involving a discrete state, whereas the other corresponds to the escape of the confined charge carrier (electron) to a (conduction) band. For the last channel, the correlation of the activation energy with structural properties allowed us to conclude that the ZB segments are wider for the growth on Si(111).

The luminescence related to the Mg was only observed from CL performed on the GaAs epilayer. For both CL and PL, no emission related to the Mg in the nanowires was found. We attribute this fact to the dominant type II character of the observed radiative transitions that masked a possible involvement of Mg acceptors in the WZ segments.

ACKNOWLEDGMENTS

This work was supported by FCT, through Projects PEst-C/CTM/LA0025/2011 and RECI/FIS-NAN/0183/2012,

[This article is copyrighted as indicated in the article. Reuse of AIP content is subject to the terms at: http://scitation.aip.org/termsconditions. Downloaded to] IP: 130.235.184.47 On: Sat, 08 Feb 2014 17:58:38

CNPq, CAPES, and FAPMIG. TEM analyses were carried out at DME, SCCYT-UCA, and supported by the Junta de Andalucía with the EU-FEDER co-funding (PAI group TEP-120 and projects P09-TEP-5403 and P08-TEP-03516) and by the CICYT project MAT 2010-15206. The CL measurements were done with support from the Swedish research council (VR). The authors would like to thank J. Coutinho for the discussion of the energy-level scheme and a careful reading of the paper.

[1]M. Koguchi, H. Kakibayashi, M. Yazawa, K. Hiruma, and T. Katsuyama, Jpn. J. Appl. Phys., Part 1 **31**, 2061 (1992).
[2]T. Martensson, C. P. T. Svensson, B. A. Wacaser, M. W. Larsson, W. Seifert, K. Deppert, A. Gustafsson, L. R. Wallenberg, and L. Samuelson, Nano Lett. **4**, 1987 (2004).
[3]F. Glas, J.-C. Harmand, and G. Patriarche, Phys. Rev. Lett. **99**, 146101 (2007).
[4]H. J. Joyce, Q. Gao, H. H. Tan, C. Jagadish, Y. Kim, J. Zou, L. M. Smith, H. E. Jackson, J. M. Yarrison-Rice, P. Parkinson, and M. B. Johnston, Prog. Quantum Electron. **35**, 23 (2011).
[5]T. Akiyama, K. Nakamura, and T. Ito, Phys. Rev. B **73**, 235308 (2006).
[6]M. Galicka, M. Bukała, R. Buczko, and P. Kacman, J. Phys.: Condens. Matter **20**, 454226 (2008).
[7]J. Johansson, L. S. Karlsson, K. A. Dick, J. Bolinsson, B. A. Wacaser, K. Deppert, and L. Samuelson, Cryst. Growth Des. **9**, 766 (2009).
[8]D. Spirkoska, J. Arbiol, A. Gustafsson, S. Conesa-Boj, F. Glas, I. Zardo, M. Heigoldt, M. H. Gass, A. L. Bleloch, S. Estrade, M. Kaniber, J. Rossler, F. Peiró, J. R. Morante, G. Abstreiter, L. Samuelson, and A. Fontcuberta i Morral, Phys. Rev. B **80**, 245325 (2009).
[9]J. Johansson, K. A. Dick, P. Caroff, M. E. Messing, J. Bolinsson, K. Deppert, and L. Samuelson, J. Phys. Chem. C **114**, 3837 (2010).
[10]M. Heiss, S. Conesa-Boj, J. Ren, H.-H. Tseng, A. Gali, A. Rudolph, E. Uccelli, F. Peiró, J. R. Morante, D. Schuh, E. Reiger, E. Kaxiras, J. Arbiol, and A. Fontcuberta i Morral, Phys. Rev. B **83**, 045303 (2011).
[11]J. C. Harmand, G. Patriarche, N. Péré-Laperne, M.-N. Mérat-Combes, L. Travers, and F. Glas, Appl. Phys. Lett. **87**, 203101 (2005).
[12]J. C. González, A. Malachias, R. R. Andrade, J. C. de Sousa, M. V. Moreira, and A. G. de Oliveira, J. Nanosci. Nanotechnol. **9**, 4673 (2009).
[13]R.-R. Andrade, A. Malachias, G. Kellerman, F. R. Negreiros, N. M. Santos, N. A. Sobolev, M. V. B. Moreira, A. G. de Oliveira, and J. C. González, J. Phys. Chem. C **116**, 24777 (2012).
[14]J. González, M. da Silva, X. Lozano, D. Zanchet, D. Ugarte, E. Ribeiro, H. Gutiérrez, and M. Cotta, J. Nanosci. Nanotechnol. **6**, 2182 (2006).
[15]V. Lopez-Richard, J. C. González, F. M. Matinaga, C. Trallero-Giner, E. Ribeiro, M. R. S. Dias, L. Villegas-Lelovsky, and G. E. Marques, Nano Lett. **9**, 3129 (2009).
[16]X.-Y. Bao, C. Soci, D. Susac, J. Bratvold, D. P. R. Aplin, W. Wei, C.-Y. Chen, S. A. Dayeh, K. L. Kavanagh, and D. Wang, Nano Lett. **8**, 3755 (2008).
[17]R. S. Wagner and W. C. Ellis, Appl. Phys. Lett. **4**, 89 (1964).
[18]M. C. Plante and R. R. LaPierre, Nanotechnology **19**, 495603 (2008).
[19]K. A. Dick, P. Caroff, J. Bolinsson, M. E. Messing, J. Johansson, K. Deppert, L. R. Wallenberg, and L. Samuelson, Semicond. Sci. Technol. **25**, 024009 (2010).
[20]H. J. Joyce, J. Wong-Leung, Q. Gao, H. H. Tan, and C. Jagadish, Nano Lett. **10**, 908 (2010).
[21]J.-M. Jancu, K. Gauthron, L. Largeau, G. Patriarche, J.-C. Harmand, and P. Voisin, Appl. Phys. Lett. **97**, 041910 (2010).
[22]U. Jahn, J. Lähnemann, C. Pfüller, O. Brandt, S. Breuer, B. Jenichen, M. Ramsteiner, L. Geelhaar, and H. Riechert, Phys. Rev. B **85**, 045323 (2012).
[23]M. Murayama and T. Nakayama, Phys. Rev. B **49**, 4710 (1994).
[24]A. De and C. E. Pryor, Phys. Rev. B **81**, 155210 (2010).
[25]S.-G. Ihn, M.-Y. Ryu, and J.-I. Song, Solid State Commun. **150**, 729 (2010).
[26]Z. Zanolli, F. Fuchs, J. Furthmüller, U. von Barth, and F. Bechstedt, Phys. Rev. B **75**, 245121 (2007).
[27]T. B. Hoang, A. F. Moses, H. L. Zhou, D. L. Dheeraj, B. O. Fimland, and H. Weman, Appl. Phys. Lett. **94**, 133105 (2009).
[28]L. Ahtapodov, J. Todorovic, P. Olk, T. Mjåland, P. Slåttnes, D. L. Dheeraj, A. T. J. van Helvoort, B.-O. Fimland, and H. Weman, Nano Lett. **12**, 6090 (2012).
[29]B. Ketterer, M. Heiss, M. J. Livrozet, A. Rudolph, E. Reiger, and A. Fontcuberta i Morral, Phys. Rev. B **83**, 125307 (2011).
[30]M. Moewe, L. C. Chuang, S. Crankshaw, C. Chase, and C. Chang-Hasnain, Appl. Phys. Lett. **93**, 023116 (2008).
[31]B. V. Novikov, S. Y. Serov, N. G. Filosofov, I. V. Shtrom, V. G. Talalaev, O. F. Vyvenko, E. V. Ubyivovk, Y. B. Samsonenko, A. D. Bouravleuv, I. P. Soshnikov, N. V. Sibirev, G. E. Cirlin, and V. G. Dubrovskii, Phys. Status Solidi RRL **4**, 175 (2010).
[32]S. A. Fortuna and X. Li, Semicond. Sci. Technol. **25**, 024005 (2010).
[33]D. Spirkoska, A. L. Efros, W. R. L. Lambrecht, T. Cheiwchanchamnangij, A. Fontcuberta i Morral, and G. Abstreiter, Phys. Rev. B **85**, 045309 (2012).
[34]A. M. Graham, P. Corfdir, M. Heiss, S. Conesa-Boj, E. Uccelli, A. Fontcuberta i Morral, and R. T. Phillips, Phys. Rev. B **87**, 125304 (2013).
[35]F. Martelli, M. Piccin, G. Bais, F. Jabeen, S. Ambrosini, S. Rubini, and A. Franciosi, Nanotechnology **18**, 125603 (2007).
[36]B. P. Falcão, J. P. Leitão, J. C. González, M. R. Correia, K. G. Zayas-Bazán, F. M. Matinaga, M. B. Moreira, C. F. Leite, and A. G. de Oliveira, J. Mater. Sci. **48**, 1794 (2013).
[37]H. J. Park, J. Kim, M. S. Kim, D. Y. Kim, J. S. Kim, J. S. Kim, J. S. Son, H. H. Ryu, G. S. Cho, M. Jeon, and J. Leem, J. Cryst. Growth **310**, 2427 (2008).
[38]C. E. C. Wood, D. Desimone, K. Singer, and G. W. Wicks, J. Appl. Phys. **53**, 4230 (1982).
[39]M. Mannoh, Y. Nomura, K. Shinozaki, M. Mihara, and M. Ishii, J. Appl. Phys. **59**, 1092 (1986).
[40]H. Kressel and F. Z. Hawrylo, J. Appl. Phys. **41**, 1865 (1970).
[41]D. J. Ashen, P. J. Dean, D. T. J. Hurle, J. B. Mullin, A. M. White, and P. D. Greene, J. Phys. Chem. Solids **36**, 1041 (1975).
[42]A. Y. Cho and M. B. Panish, J. Appl. Phys. **43**, 5118 (1972).
[43]D. Rudmann, D. Brémaud, A. F. da Cunha, G. Bilger, A. Strohm, M. Kaelin, H. Zogg, and A. N. Tiwari, Thin Solid Films **480–481**, 55 (2005).
[44]M. G. Sousa, A. F. da Cunha, P. M. P. Salomé, P. A. Fernandes, J. P. Teixeira, and J. P. Leitão, Thin Solid Films **535**, 27–30 (2013).
[45]E. Uccelli, J. Arbiol, C. Magen, P. Krogstrup, E. Russo-Averchi, M. Heiss, G. Mugny, F. Morier-Genoud, J. Nygård, J. R. Morante, and A. Fontcuberta i Morral, Nano Lett. **11**, 3827 (2011).
[46]E. Russo-Averchi, M. Heiss, L. Michelet, P. Krogstrup, J. Nygård, C. Magen, J. R. Morante, E. Uccelli, J. Arbiol, and A. Fontcuberta i Morral, Nanoscale **4**, 1486 (2012).
[47]E. Bakkers, M. Borgström, and M. Verheijen, MRS Bull. **32**, 117 (2007).
[48]A. Belabbes, C. Panse, J. Furthmüller, and F. Bechstedt, Phys. Rev. B **86**, 075208 (2012).
[49]*PDF 04-003-3796* (ICDD, 1973).
[50]*PDF 01-080-0003* (ICDD, 2010).
[51]C.-Y. Yeh, Z. W. Lu, S. Froyen, and A. Zunger, Phys. Rev. B **46**, 10086 (1992).
[52]A. Gustafsson, M.-E. Pistol, L. Montelius, and L. Samuelson, J. Appl. Phys. **84**, 1715 (1998).
[53]E. H. Bogardus and H. B. Bebb, Phys. Rev. **176**, 993 (1968).
[54]L. Pavesi and M. Guzzi, J. Appl. Phys. **75**, 4779 (1994).
[55]K. Tomioka, Y. Kobayashi, J. Motohisa, S. Hara, and T. Fukui, Nanotechnology **20**, 145302 (2009).
[56]T. Schmidt, K. Lischka, and W. Zulehner, Phys. Rev. B **45**, 8989 (1992).
[57]G. Jacopin, L. Rigutti, L. Largeau, F. Fortuna, F. Furtmayr, F. H. Julien, M. Eickhoff, and M. Tchernycheva, J. Appl. Phys. **110**, 064313 (2011).
[58]M. Wachter, K. Thonke, R. Sauer, F. Schäffler, H.-J. Herzog, and E. Kasper, Thin Solid Films **222**, 10 (1992).
[59]P. Boucaud, S. Sauvage, M. Elkurdi, E. Mercier, T. Brunhes, V. Le Thanh, D. Bouchier, O. Kermarrec, Y. Campidelli, and D. Bensahel, Phys. Rev. B **64**, 155310 (2001).
[60]M. W. Dashiell, U. Denker, and O. G. Schmidt, Appl. Phys. Lett. **79**, 2261 (2001).
[61]Y. Chen, B. Pan, T. Nie, P. Chen, F. Lu, Z. Jiang, and Z. Zhong, Nanotechnology **21**, 175701 (2010).
[62]C. Weisbuch and B. Vinter, *Quantum Semiconductor Structures* (Academic Press, Boston, 1991).

[This article is copyrighted as indicated in the article. Reuse of AIP content is subject to the terms at: http://scitation.aip.org/termsconditions. Downloaded to] IP: 130.235.184.47 On: Sat, 08 Feb 2014 17:58:38

[63]Y. S. Chiu, M. H. Ya, W. S. Su, and Y. F. Chen, J. Appl. Phys. **92**, 5810 (2002).
[64]Y. I. Mazur, V. G. Dorogan, G. J. Salamo, G. G. Tarasov, B. L. Liang, C. J. Reyner, K. Nunna, and D. L. Huffaker, Appl. Phys. Lett. **100**, 033102 (2012).
[65]P. J. Simmonds, R. B. Laghumavarapu, M. Sun, A. Lin, C. J. Reyner, B. Liang, and D. L. Huffaker, Appl. Phys. Lett. **100**, 243108 (2012).
[66]N. Pavarelli, T. J. Ochalski, F. Murphy-Armando, Y. Huo, M. Schmidt, G. Huyet, and J. S. Harris, Phys. Rev. Lett. **110**, 177404 (2013).
[67]M. L. W. Thewalt, D. A. Harrison, C. F. Reinhart, J. A. Wolk, and H. Lafontaine, Phys. Rev. Lett. **79**, 269 (1997).
[68]M. Jo, M. Sato, S. Miyamura, H. Sasakura, H. Kumano, and I. Suemune, Nanoscale Res. Lett. **7**, 654 (2012).
[69]V. Fiorentini, F. Bernardini, F. Della Sala, A. Di Carlo, and P. Lugli, Phys. Rev. B **60**, 8849 (1999).
[70]Z. Vashaei, C. Bayram, P. Lavenus, and M. Razeghi, Appl. Phys. Lett. **97**, 121918 (2010).
[71]J. Lähnemann, O. Brandt, C. Pfüller, T. Flissikowski, U. Jahn, E. Luna, M. Hanke, M. Knelangen, A. Trampert, and H. T. Grahn, Phys. Rev. B **84**, 155303 (2011).
[72]R. Pässler, Phys. Status Solidi B **200**, 155 (1997).
[73]S. D. Singh, S. Porwal, K. Alexander, V. K. Dixit, A. K. Srivastava, and S. M. Oak, J. Phys. D: Appl. Phys. **43**, 455410 (2010).
[74]J. P. Leitão, A. Carvalho, J. Coutinho, R. N. Pereira, N. M. Santos, A. O. Ankiewicz, N. A. Sobolev, M. Barroso, J. L. Hansen, A. N. Larsen, and P. R. Briddon, Phys. Rev. B **84**, 165211 (2011).

[This article is copyrighted as indicated in the article. Reuse of AIP content is subject to the terms at: http://scitation.aip.org/termsconditions. Downloaded to] IP: 130.235.184.47 On: Sat, 08 Feb 2014 17:58:38